

# Genetic algorithm based energy-saving ATO control algorithm for CBTC

Zheng Wang<sup>1</sup>, Xiangxian Chen<sup>1, \*</sup>, Hai Huang<sup>1</sup>, Yue Zhang<sup>2</sup>

<sup>1</sup>Department of Instrument Science and Engineering, Zhejiang University, Hangzhou, China

<sup>2</sup>Southwest China Research Institute of Electronic Equipment, Chengdu, China

To improve their carrying capacities, multiple trains can operate on one line. Urban rail transit employs a Communication-Based Train Control (CBTC) system to realize a movable block, which is applied to decrease the headway. In a CBTC system, trains only know the speed limit within the scope of the Movement Authority Limit (MAL). An energy-saving Automatic Train Operation (ATO) control algorithm based on a genetic algorithm (GA) is proposed to control multi-train movements with incomplete information about speed limits. This algorithm is composed of two layers: a search layer that applies a GA to search for the optimal control solution and a protection layer that helps trains prevent overspeed. The GA in this paper tends to achieve optimal solutions using variable length chromosomes and a novel fitness function. The simulation results indicate that the proposed algorithm achieves optimal energy-saving benefits compared with other control strategies.

Keywords: CBTC, energy-saving, genetic algorithm, automatic train operation

## 1. INTRODUCTION

Urban rail transportation requires trains to be safe, speedy, efficient and punctual. To achieve these goals, an Automatic Train Control (ATC) system has been extensively applied. An ATC system consists of three subsystems: the Automatic Train Supervision (ATS) system, the Automatic Train Protection (ATP) system and the Automatic Train Operation (ATO) system. The ATS system is employed in a control center and generates all control instructions. The ATP system is a safety-critical system that prevents trains from overspeed and other hazards. The ATO system receives information from other systems, such as the ATP system, and controls the operation of a train instead of the driver of a train.

The majority of ATO systems in service have adopted conventional algorithms, such as a PID algorithm, or improved versions of these algorithms. Use of the PID algorithm to control train movement introduces some disadvantages, such as con-

tinual switchovers between acceleration and deceleration. The PID algorithm has a negative effect on the ride performance, ride comfort and energy consumption of a train. To improve the performance of ATO systems, research on the control algorithms applied in ATO systems has been performed with satisfactory outcomes. Wang applied iterative learning control to effectively track the guidance trajectory without deviation after repeating the same trip a sufficient number of times [1]. Sekine proposed a two-degree-of-freedom fuzzy neural network control system to operate a train according to the generated reference patterns [2]. Oshima presented a predictive fuzzy control algorithm to select a control rule with a maximum comprehensive membership value as the output to control a train [3]. Gao proposed a fuzzy-PID switching control to improve the accuracy and response of the ATO system [4] and developed a fuzzy control algorithm using the adaptive quantization factor and scale factor [5]. Chang and his colleagues tuned a fuzzy ATO according to current operating conditions to solve a multi-objective problem, including punctuality, ride comfort and energy consumption, using differential evolution and the Pareto-optimal set [6, 7]. Chang and Han pro-

\*Corresponding author. E-mail: xxchen99@zju.edu.cn

posed optimal methods using a GA to search for the appropriate coast control table [8, 9]. Bocharnikov also presented the ATO system based on a GA, which selects novel genes of acceleration rate, deceleration rate and the rate of minimum and maximum coasting speeds [10]. Domínguez and her colleagues designed an accurate and realizable simulation model to achieve the optimal ATO speed profile [11]. Thomas Albrecht used a GA to search for an optimal distribution of a train's running time reserve to enhance the utilization rate of the energy generated by regenerative braking [12].

During a single-train journey, the ATO system is permitted to consider civil speed limits in the track database as speed limits. In this situation, presuming that the wayside equipment is in a certain state, the ATO system can acquire all speed limits between two stations. In an actual situation, however, multiple trains always exist in a certain rail line for efficiency. In addition, the states of wayside equipment are variable (for example, the position of the track switches change between the normal position and the reverse position for different routes of trains). Baek employed a beacon to derive a new algorithm to realize trains' separation control in [18, 19]. Gao demonstrated adaptive coordination control of trains by train-to-train communication [20]. Takagi presented the synchronization control of trains in a line of a moving block signaling system [21]. In a Communication Based Train Control (CBTC) system, zone controllers distribute a Movement Authority Limit (MAL) to each train according to the headway, track occupancy and track state. Then, the ATP system calculates speed limits within the scope of the MAL, and speed limits beyond the scope of the MAL are unknown. Thus, only a part of the information of interstation speed limits is known. Although they are applied to the situation in which incomplete information about speed limits, the ATO systems in service, such as the PID algorithm-based systems, the predictive fuzzy control algorithm-based system proposed by Oshima [3], the fuzzy train tracking algorithm presented by Carvajal [22, 26], the simulation algorithm developed by Ding [23], the smoothing technique demonstrated by Gu [24] and the mixed integer linear programming designed by Wang [25], have to be configured with particular parameters to be punctual and energy-efficient for particular situations using methods such as heuristics and trial and error. However, these systems cannot minimize the energy consumption using the configured parameters because conditions (such as speed limits and train loads) that affect the configuration of the parameters vary by journey. Although numerous energy-saving algorithms exist, such as [17, 23, 24, 26, 28], they cannot be applied to train operation or have some of the previously mentioned disadvantages. Instead of configuring the parameters to situations that differ from actual situations, a GA can search the optimal energy-saving control strategy according to the actual conditions of every train journey. It can provide a global approach for train control. However, research about GA-based ATO systems have always been conducted in situations in which all speed limits are known [8–10].

The main contribution of this paper is to propose an energy-saving ATO control algorithm that is based on a GA to control multi-train movements with a CBTC system for the situation in which all speed limits are not known. The algorithm uses three operation modes to control trains: traction mode, coasting mode and braking mode. We assume that the traction mode has the highest grade, the coasting mode has a lower grade and the

braking mode has the lowest grade. The proposed algorithm consists of two layers: a search layer and a protection layer. The search layer uses a GA to search for the optimal control solution to determine the position where coasting should start or terminate. The protection layer prevents a train from overspeed by degrading the operation mode when the train speed exceeds the speed limit. This algorithm employs the permitted maximum acceleration and deceleration and coasting to minimize energy consumption. The implementation of the proposed ATO control algorithm is detailed, and the performance of the proposed algorithm is compared with the performance of the algorithms that employ other strategies.

The incomplete speed limits, train modeling and control strategy are described in Section 2. The energy-saving ATO algorithm is detailed in Section 3. Section 4 describes the simulation, and the results are discussed. The conclusions are presented in Section 5.

## 2. PREMISE AND STRATEGY

### 2.1 Incomplete Speed Limits Information

The ATO system obtains the speed limit of the current position from the ATP system. This speed limit is referred to as the current speed limit. The ATO system obtains information about the speed limits within the scope of the MAL from the ATP system, receives information about the next stop station and the schedule time from the ATS system, and collects gradient and curve information from the track database. Considering this information, the ATO system outputs a control proportion that ranges from  $-100\%$  to  $100\%$  to the train to control its movement (negative and positive proportion represent the braking mode and the traction mode respectively, and the absolute value of the proportion represents the rate that the force accounts for the maximum force and determines the value of acceleration or deceleration.  $0\%$  denotes the coasting mode). The data stream is illustrated in Figure 1.

In an actual train journey, the ATO system can only operate the train under the protection of the ATP system, that is, it can only acquire the speed limit within the scope of the MAL. We refer to the point where the speed limit changes the target point and consider the zone between two target points as one section. The speed limit information within the scope of the MAL has two types of states: change points where civil speed limits are included or change points where civil speed limits are not included. The definition of a target point and a section of the two states are illustrated in Figure 2(a) and Figure 2(b). The proposed algorithm sets a section as the working range, uses the current speed limit, the speed limit of the target point, the location of the target point, and the schedule time and information of the gradient and curve as inputs and outputs a proportion to control the train.

### 2.2 Train Model

#### 2.2.1 Non-Particle Model

The general approach of a modeling train is referred to as a single-particle model, where the train is considered to be a sin-

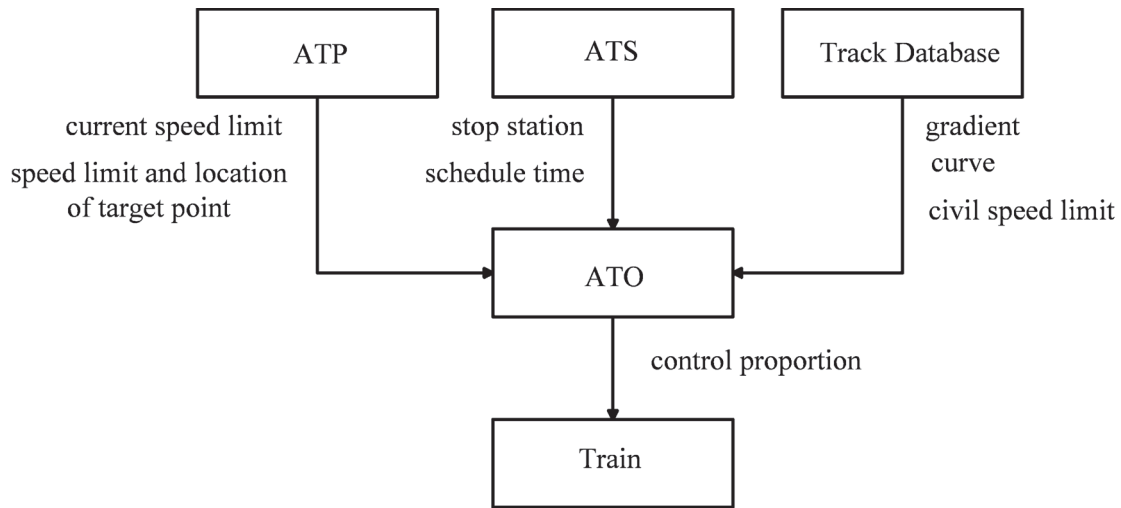


Figure 1 Data stream.

gle particle [15]. Few studies employ this method due to its large error in calculating additional resistances, especially resistance caused by the gradient. In a multi-particle model, every carriage of a train is regarded as a particle without considering the carriage length [16, 27]. In this paper, a non-particle model is proposed, and additional resistance due to the gradient is periodically calculated with the carriage length according to (2.1), where  $i_{rgj}$  is the additional resistance due to the gradient of the  $j$ th carriage,  $g_{pre}$  is the gradient before it changes for the  $j$ th carriage,  $g_{post}$  is the changed gradient,  $l$  is the length of the  $j$ th carriage on the changed gradient ( $m$ ), and  $L$  is the length of the  $j$ th carriage ( $m$ ). The carriage that crosses over different gradients is shown in Figure 3. Figure 4 shows some curves of additional resistance due to the gradient calculated by different approaches. The curve of the non-particle model looks more natural because its changes are smooth compared with the sharp or stepped curves of the other two models.

$$i_{rgj} = g_{post} \frac{l}{L} + g_{pre} \left( \frac{L-l}{L} \right) \quad (2.1)$$

### 2.2.2 Time Delay and jerk Limit

The commands need the time slot  $T_{tr}$  to be transferred from the ATO control system to the response of the motor. If the command is directly changed from traction mode (brake) to brake mode (traction), the motor would not work for a time slot, which is termed as  $T_{dead}$ . When a train is coasting, its motor is idle. Therefore, if the command is changed from coast to brake (traction), the motor needs the time slot,  $T_{up}$  to start to work again. Considering the comfortability, the motor also has a limit of the derivative of the acceleration rate, which is termed  $jerk$ ; the maximum absolute value of the derivative of acceleration or deceleration should be less than  $jerk$ . The control changes according to  $jerk$  and needs a time slot, which is termed as  $T_{jerk}$ . Figure 5 depicts the entire procedure of time delay when the ATO system outputs a command to change the control from traction to brake,

where  $I_q$  is the torque current, and the real effect of a train to the command.

### 2.2.3 Identifying parameters with GA

In addition to the previously mentioned factors, some other factors influence the train model, such as the kinetic parameters, traction, brake, basic resistance and additional resistance (including slopes, curves and tunnels); these are empirical data. A train system is a highly coupled system due to its high safety and operation environment. Many of the previously mentioned factors are indeterminate and experimental. Thus, the trains that are only modeled by empirical data are general, and many errors will occur if the models are applied to all types of accurate studies. The train model in this paper is constructed by an identification approach with GA, where  $T_{dead}$ ,  $T_{tr}$ ,  $T_{up}$ ,  $jerk$ , traction, brake, basic resistance, additional resistance, and the inertia factor are employed as identification indices. We regard the nine parameters as nine genes of a chromosome and search the best chromosome as the optimal solution with a GA, based on real data from the onsite records. Therefore, we can construct a precise model of the train by the optimal solution, which is suitable for a specific type of train, namely, a specific model.

In the modeling process, the actual input commands of a train are employed as a reference. The fitness function completes the simulation of a series of activities after the train obtain commands from the ATO or controlling system. The results of the commands are presented by the change in velocity and displacement. In contrast with the real recorded velocity, we can obtain the similarity of the simulation data and determine the fitness of every chromosome. The closer are the two speeds, the smaller is the objective function value, and the larger is the fitness of the chromosome. The flow chart of the fitness function is shown in Figure 6.

Some simulation results, which can prove the accuracy of the train model, are provided in Section 4. The ATO control algorithms in this paper simulate using the previously described train model.

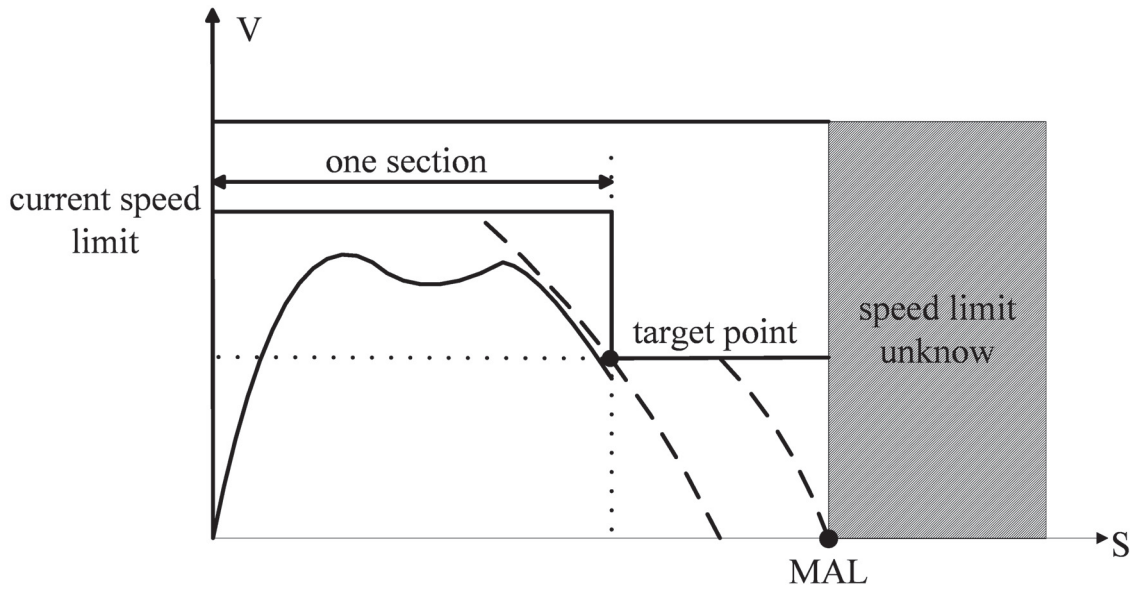


Figure 2 (a) Change point of civil speed limit is included within MAL scope.

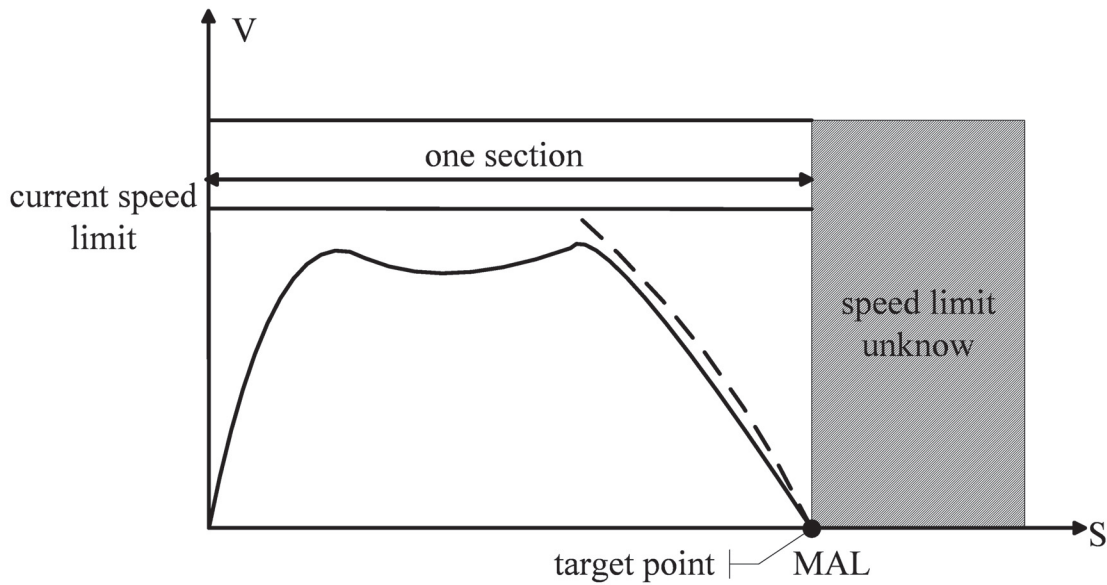


Figure 2 (b) No change point of civil speed limit within MAL scope.

### 2.3 Control Strategy

A flat-out operation employs the maximum permitted traction force or braking force when the traction mode or braking mode is applied and implements uniform motion (cruise) when the train speed reaches the speed limit (usually a lower speed limit causes a certain margin to avoid overshooting, which will trigger the emergency brake (EB)). The scheduled time always exceeds the pure run-time of a flat-out operation; it is typically greater by 15% [13]. To consume the extra time of the schedule, strategies such as reducing the control proportion and cruising speed can be employed, as shown in Figure 7. Our research indicates that the strategy of reducing the control proportion consumes more energy than the strategy of reducing the cruising speed. The process of cruising mode can be replaced by the alternate implementation of traction mode and coasting mode, as shown

in Figure 7. In this approach, energy can be saved and frequent switchover can be avoided.

### 3. THE ENERGY-SAVING ATO ALGORITHM BASED ON GA

The application of coasting mode can save energy, make a train punctual and avoid frequent switchover. A GA offers a feasible approach to solve this multi-objective problem. This paper proposes an energy-saving ATO control algorithm that is based on a GA. This algorithm is composed of two layers: a search layer that applies a GA to search for the optimal control solution and a protection layer that prevents the train from overspeed.

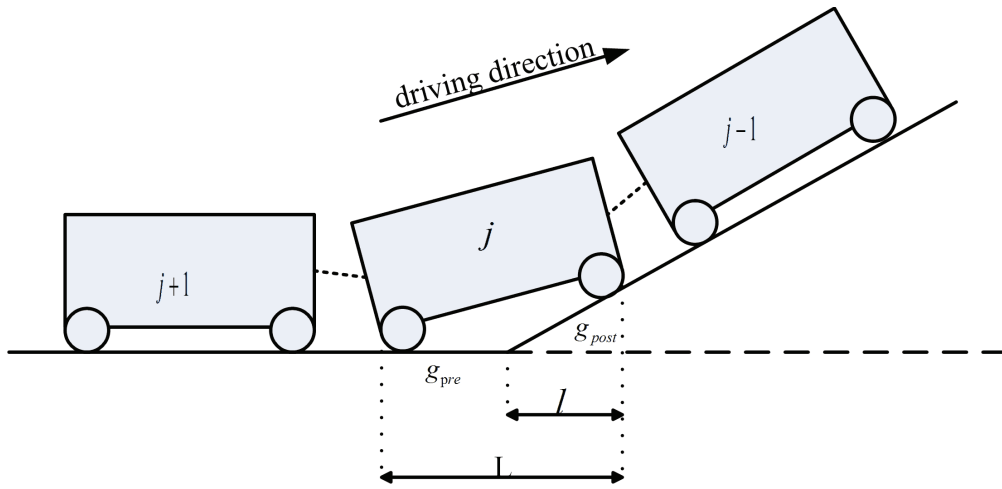


Figure 3 Gradient changes.

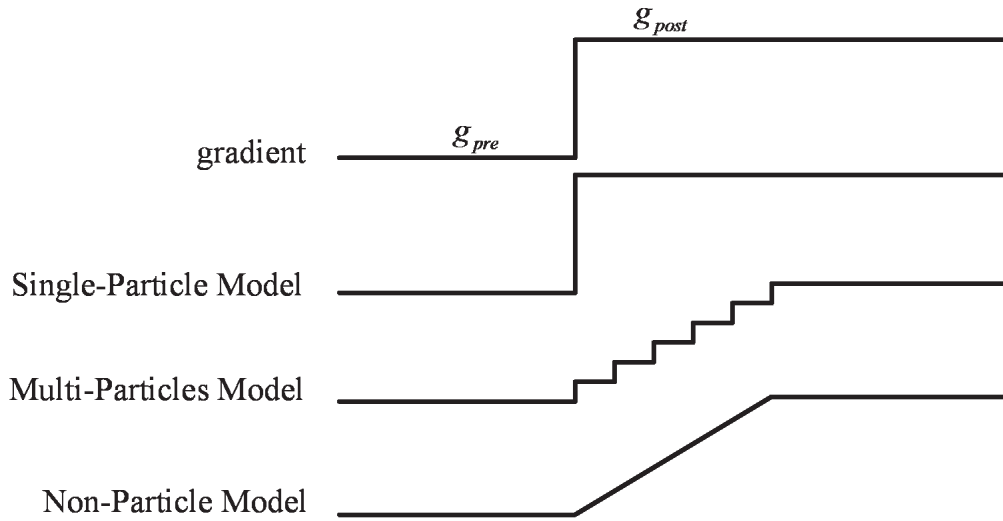


Figure 4 Curves of additional resistance due to the gradients in different models.

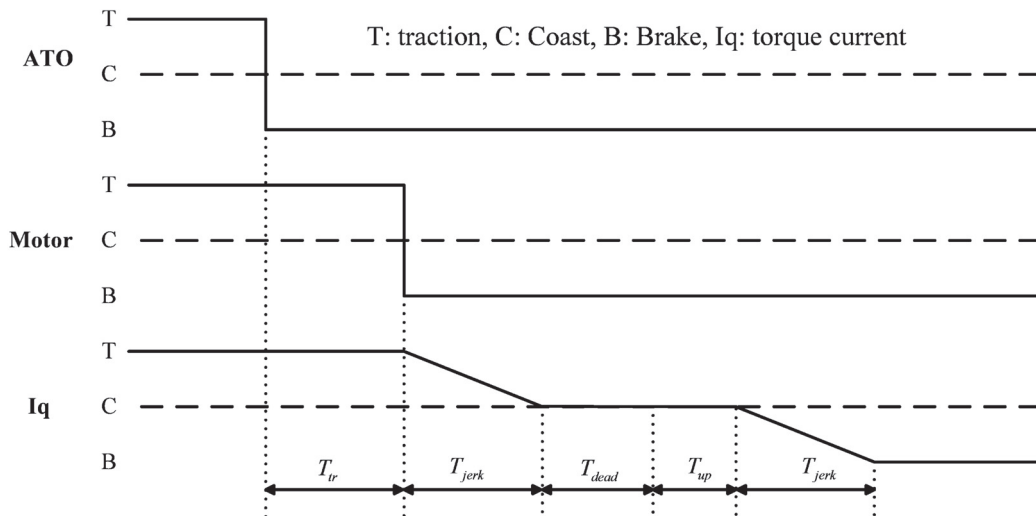


Figure 5 Time delay from the ATO output command to the train response.

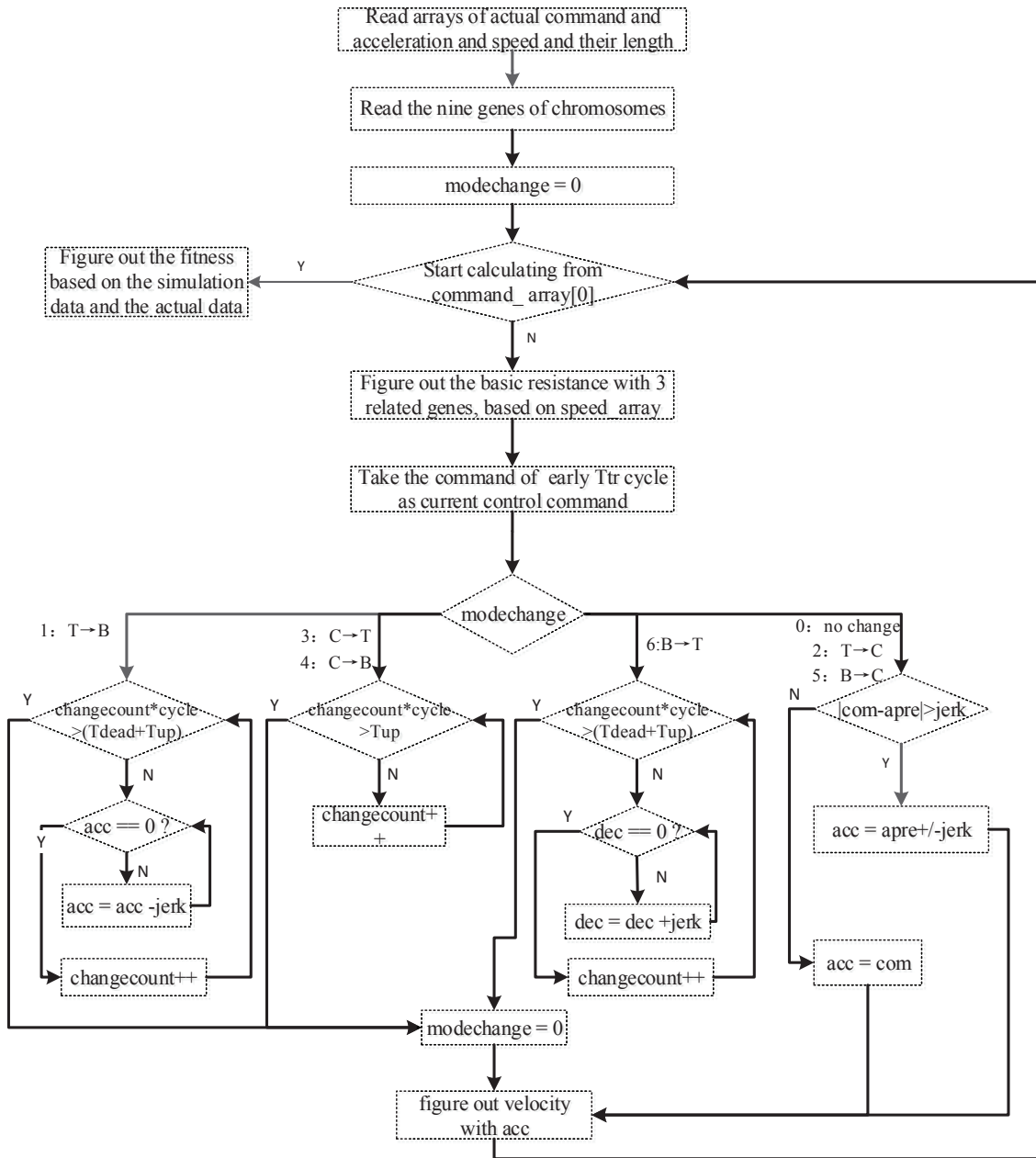


Figure 6 Flow chart of fitness function.

### 3.1 Search Layer Based on GA

#### 3.1.1 Design of Chromosome

The genes of a chromosome represent the positions where the coasting mode starts or terminates. Using the centimeter as the unit of position enables a train to stop within 30 cm, and coding the chromosome in real numbers increases the search efficiency. The genes in a chromosome are in ascending order. The values of genes at an odd locus (the position of a gene in a chromosome) represent the starting positions of the coasting mode, whereas the values of genes at an even locus represent the starting positions of the traction mode. For example, a chromosome with four genes that range in ascending order,  $g_1g_2g_3g_4$ , represents that the coasting mode will be implemented when the train's position

is  $g_1$  or  $g_3$  and the traction mode will be implemented when the train is at the point  $g_2$  or  $g_4$ . The starting point of a section is denoted as  $g_0$ . If the train speed is 0 m/s or the difference between the speed limit and the train speed is large (larger than 1.4 m/s), the traction mode will be chosen; otherwise, the coasting mode is chosen. Different sections have different lengths, speed limits and schedules. Use of variable-length chromosomes renders the algorithm more flexible.

#### 3.1.2 Genetic Operation

The proposed GA contains six operations: (1) reproduction, which employs tournament selection; (2) crossover, which needs the chromosomes of the same length to be paired; (3) mutation; (4) gene duplications; (5) gene deletions and (6) elitist selection.

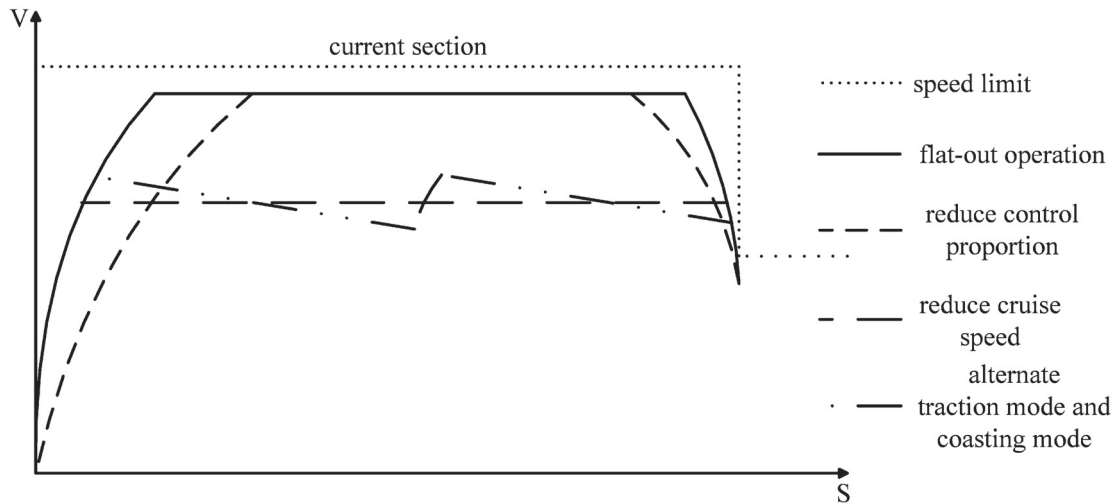


Figure 7 Strategies applied in a section.

Operations (1) – (3) belong to conventional genetic operations [14], whereas operations (4) and (5) generate chromosomes of different lengths. If the length of a chromosome is smaller than seven, a randomly generated new gene will be appended to the chromosome at a certain probability. If the length of a chromosome is larger than one, the gene at a random locus of this chromosome will be deleted at a certain probability. Operation (6) is used to accelerate the convergence of the algorithm by retaining the chromosome with the best performance. At the end of each operation, the genes should be arranged in ascending order.

### 3.1.3 Fitness Function

**Penalty Functions Comes from Constraints** The following constraints should be obeyed during the entire train journey:

$$V \leq V_{\text{CurrentLimit}} - V_{\text{margin}} \quad (3.2)$$

$$V_t \leq V_{\text{TPLimit}} \quad (3.3)$$

$$|S_{\text{section}}| \leq 30(\text{cm}) \quad (3.4)$$

$$t = t_{\text{section}} \quad (3.5)$$

where  $V$  is the train speed (m/s),  $V_t$  is the train speed at the end of the section (m/s),  $V_{\text{CurrentLimit}}$  is the current speed limit of the ATP system (m/s),  $V_{\text{margin}} = 1.4$  m/s is the margin speed (m/s),  $V_{\text{TPLimit}}$  is the speed limit of the target point (m/s),  $S$  is the distance that the train has travelled (cm),  $S_{\text{section}}$  is the length of the section (cm),  $t$  is the run time of a train (s), and  $t_{\text{section}}$  is the schedule time of a section (s), which is 15% greater than the pure run time of the section.

The protection layer maintains the train speed under the speed limit in Formula (3.1) during the entire journey. Formulas (3.2)–(3.4) can be satisfied by screening the chromosomes with the end speed penalty  $P_{vt}$ , distance penalty  $P_s$  and punctuality penalty  $P_t$ .  $P_{vt}$ ,  $P_s$  and  $P_t$  are defined in Formulas (3.5)–(3.7).

$$P_{vt} = \begin{cases} V_{\text{TPLimit}} - V_t, & V_{\text{TPLimit}} \geq V_t \\ (V_{\text{TPLimit}} - V_t)^2, & V_{\text{TPLimit}} < V_t \end{cases} \quad (3.5)$$

$$P_s = \begin{cases} 0, & |S_{\text{section}} - S| \leq 30 \\ (S_{\text{section}} - S - 30)^2, & |S_{\text{section}} - S| > 30 \end{cases} \quad (3.6)$$

$$P_t = (t_{\text{section}} - t)^2 \quad (3.7)$$

### Fitness Function Improvement According to Performance Requirement

In addition to obeying the previous constraints, the algorithm is expected to be energy-saving and comfortable. The operation mode is seldom switched when the proposed algorithm employed. The ride comfort is guaranteed by limiting the maximum value and the change rates of the acceleration and the deceleration.

The energy consumption during a train journey includes three parts: (i) the energy consumed to accelerate a train during traction mode; (ii) the train's demand to power the equipment, such as lights; and (iii) the energy consumed for the shunting operation. Usage of regenerative braking can retrieve the energy generated by motor reversal. The energy of regenerative braking can be fed to the overhead line or stored by the capacitance or flywheel. However, the energy consumption of Part (i) is the only part that can be decreased using the optimal control strategy. Thus, it is the only part that we need to consider. The energy consumption is the accumulation of the power when the train is in the traction mode, which is defined as

$$E = \sum F_t \times V \times \Delta t \quad (3.8)$$

where  $F_t$  is the tractive force (kN).

Our research has indicated that, the fitness function, if it only consists of  $P_{vt}$ ,  $P_s$ ,  $P_t$  and  $E$ , tends to cause a control solution that generates a speed-distance profile that is similar to the bad profile shown in Figure 8. The traction time of the bad profile is longer than the good profile, which is also shown in Figure 8; that is, the bad profile indicates that the train consumes more energy than the train in the good profile. Figure 9 explains why the search result is similar to the bad profile. The outputted control sequences of the search layer contain the modes of traction and coasting, and the protection layer will not implement braking unless the train experiences overspeed. We assume that a train needs cruising at  $V_{\text{ave}}$  from point A to be punctual. If the actual train speed is  $V_1$  when the train arrives at point A, even if it has stopped accelerating, the average speed from point A to the

stop point is faster than  $V_{ave}$ , which indicates that the train will be ahead of schedule. Although it is energy-efficient, the good profile has a large penal value from  $P_s$  and is prone to screening during the iterative process of the GA. Although the bad profile has poor energy efficiency, it is punctual and has a better fitness than the good profile.

From Figure 8, we can infer that the variance of the speed of the good profile and the cruising speed is smaller than the variance of the speed of the bad profile and the cruising speed. Thus, we introduce the novel performance index  $VAR$  to improve the fitness function.  $VAR$  is the sum of the variance when the coasting mode is implemented. The definition of  $VAR$  is

$$VAR = \sum_{\text{coast}} \left( \frac{V - V_{\text{cruise}}}{V_{\text{cruise}}} \right)^2 \quad (3.9)$$

where  $V_{\text{cruise}}$  is the cruising speed of the train to be punctual (m/s). Adding this performance index to the fitness function can increase the survival rate of the chromosomes that make the train run near the good profile.

The fitness function can be concluded as follows:

$$\text{fitness} = \frac{1}{\omega_1 E + \omega_2 VAR + \beta_{vt} P_{vt} + \beta_s P_s + \beta_t P_t} \quad (3.10)$$

where  $\omega_1, \omega_2, \beta_{vt}, \beta_s$  and  $\beta_t$  represent the weight of each performance index or penalty factor.  $\beta_{vt}, \beta_s$  and  $\beta_t$  have relatively large values to screen the chromosome that breaks the constraints.

When using Formula (3.10) to calculate the fitness of a chromosome, the larger is the fitness value is, the better are the control performances of the chromosome.

### 3.2 Protection Layer

#### 3.2.1 Calculation of the Speed Limit Profile

The ATO system receives information about the speed limit from the ATP system. A margin speed (typically 1.4 m/s) should be subtracted from the current speed limit to avoid overshooting of the train speed that will trigger the EB. This is the first part of the speed limit profile. When the speed limit of the target point is lower than the current speed limit, the train should decelerate before entering the next section to avoid overspeed. A deceleration profile is calculated as the second part of the speed limit profile. Each point of the profile has paired information of speed and distance. For example, the point P shown in Figure 10 has the speed  $V_p$  and the distance  $S_p$ . The train with the speed  $V_p$  would be less than the speed limit at the entrance of the next section if it starts braking from the position  $S_p$  with the maximum deceleration. The speed limit profile combines these two parts, as illustrated in Figure 10.

#### 3.2.2 Overspeed Protection

The ATP system protects a train from overspeed and will activate the EB once the train overspeeds; the EB will not be released until the train stops. The protection of the ATP system yields poor operation performance. Thus, we design the protection layer of the ATO control algorithm to protect the train. The protection layer guarantees that all control solutions outputted from the ATO system will not trigger the EB.

The operation modes in this algorithm contain traction mode, coasting mode and braking mode. We assume that traction mode has the highest grade, coasting mode has a lower grade and braking mode has the lowest mode. The protection layer works in the following steps.

- 1) The protection layer searches for the operation mode determined by the search layer, and calculates the train speed after one second;
- 2) The protection layer compares the train speed calculated from step 1) with the speed limit after one second. If the train speed is higher, the protection layer will degrade the operation mode and continue to step 3); otherwise, it will output the operation mode to the train;
- 3) If the degraded operation mode from step 2) is coasting mode, the protection layer will calculate the train speed after one second using the degraded operation mode and continue to step 4); otherwise, it will output the degraded operation mode (the braking mode) to the train;
- 4) The protection layer compares the train speed from step 3) with the speed limit after one second. If the train speed is lower, the protection layer will output the degraded operation mode (coasting mode) to the train; otherwise, it will degrade the operation mode, and output it (braking mode) to the train.

The protection layer degrades the operation mode to prevent the train from overspeed. If the protection layer degrades the operation mode, the protection layer gains the right of control. Otherwise, the search layer gains the right of control. If the protection layer seizes the right of control from the search layer, the search layer is not allowed to regain the right of control until the train speed is 1.4 m/s slower than the speed limit. It avoids the frequent switchover of operation mode.

### 3.3 The Integrated ATO Control Algorithm

The integrated ATO control algorithm combines the protection layer and the search layer and operates a train as illustrated in Figure 12. The search layer outputs the fittest chromosome  $g1g2g3$ . The train accelerates from  $g0$ , which is the start position of the section. When the train travels to position  $g1$ , the traction is cut off and the coasting mode is released. The train accelerates when its relative position is  $g2$  and continues to accelerate until the protection layer seizes the right of control at  $p1$ . When the train travels to  $p2$ , where the speed of the train is 1.4 m/s slower than the speed limit, the search layer regains the right of control and implements the coasting mode, which should have been implemented at  $g3$ . The coasting mode continues until the speed of train exceeds the speed limit at  $p3$ . The protection layer implements the braking mode from  $p3$  to prevent the train from overspeed when it enters the next section.

## 4. SIMULATION AND RESULTS

The distribution of the gradient is shown in Figure 13. The parameters for the train are listed in Table 1, and the parameters for multi-trains are listed in Table 2.

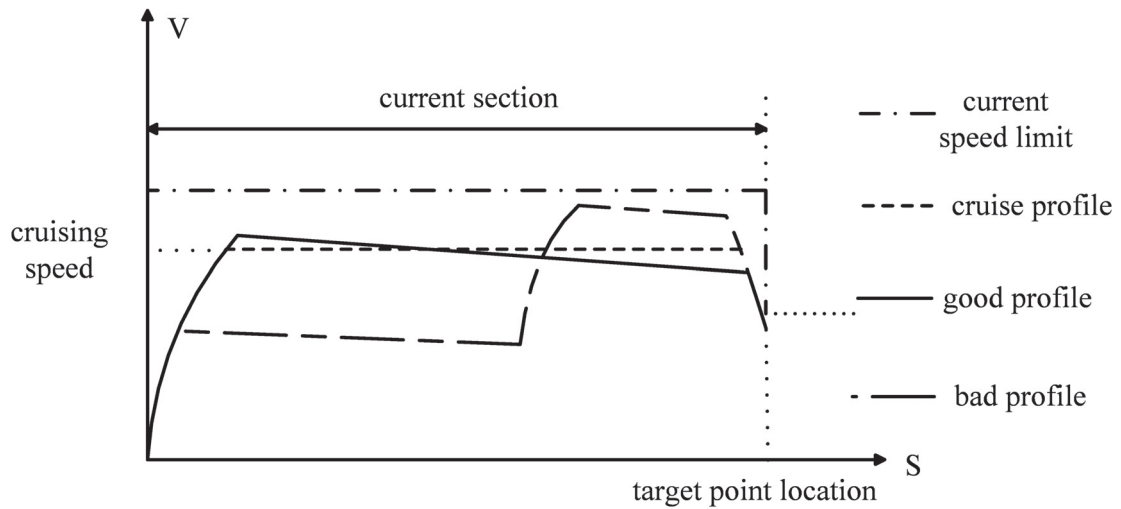


Figure 8 Good and bad speed-distance.

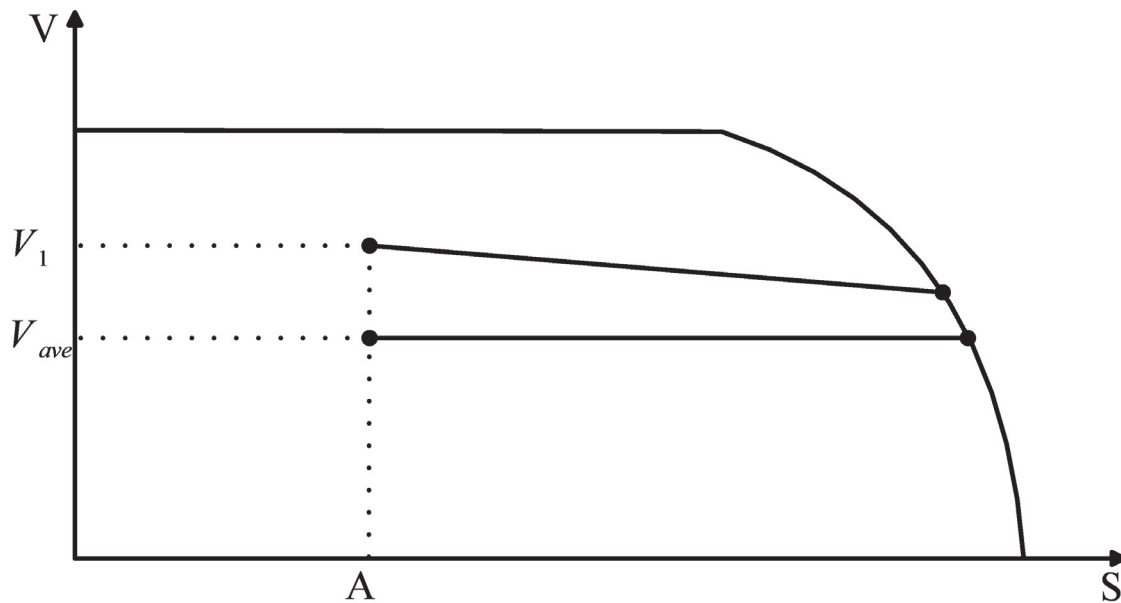


Figure 9 Reason of the appearance of the bad profile.

Table 1 Parameters for the train.

Parameter	Value
Train type	SS1 Electric-locomotive, 2 trailer 4 motor
Mass	[34.90,38.80,38.80,38.80,38.80,34.90] t
Max Passenger Load	[24.00,24.90,24.90,24.90,24.90,24.00] t
Cab-Dis(from cab-center to train head)	[1011,3000,4954,6906,8860,10849] cm
Cab Length avg	1976 cm
Rotary coefficient	0.06
Max tract force	367.11 kN
Max break force	-384.11 kN

Figure 14 and Figure 15 shows the comparison between train model data and real train operation data for speed and acceleration, respectively. Figure 14 shows that the simulation speed corresponds with the real speed. Figure 15 indicates that the delay of the actual acceleration is similar to the delay of the control;

that is, the time delay mentioned in Section 2.2.2 corresponds with the simulation acceleration and actual acceleration. These results demonstrate that our train model is very close to the real train and can replace the real train to be applied by the ATO control algorithms in this paper.

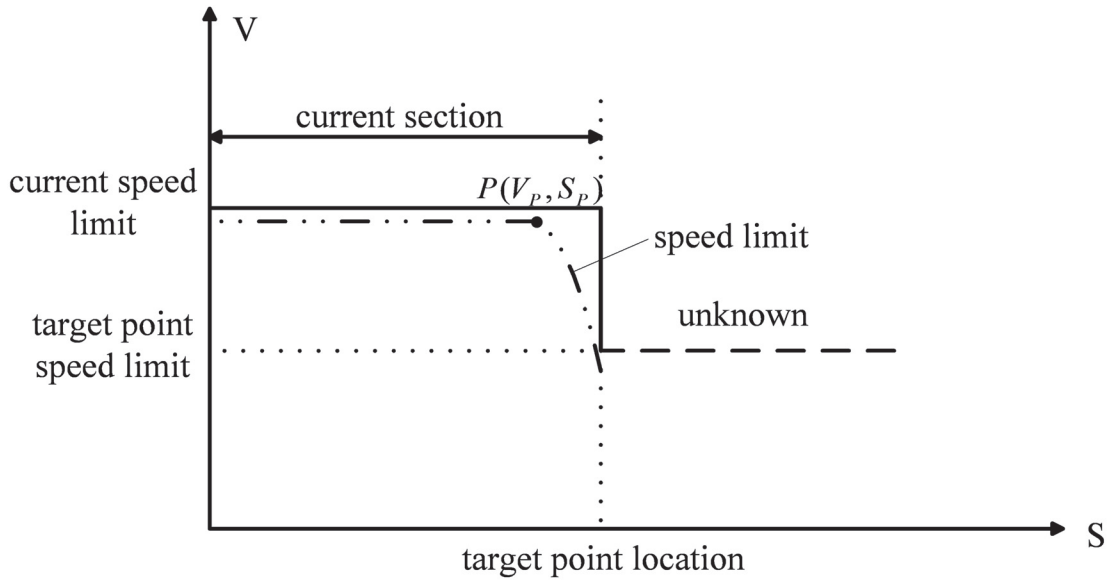


Figure 10 Speed limit profile.

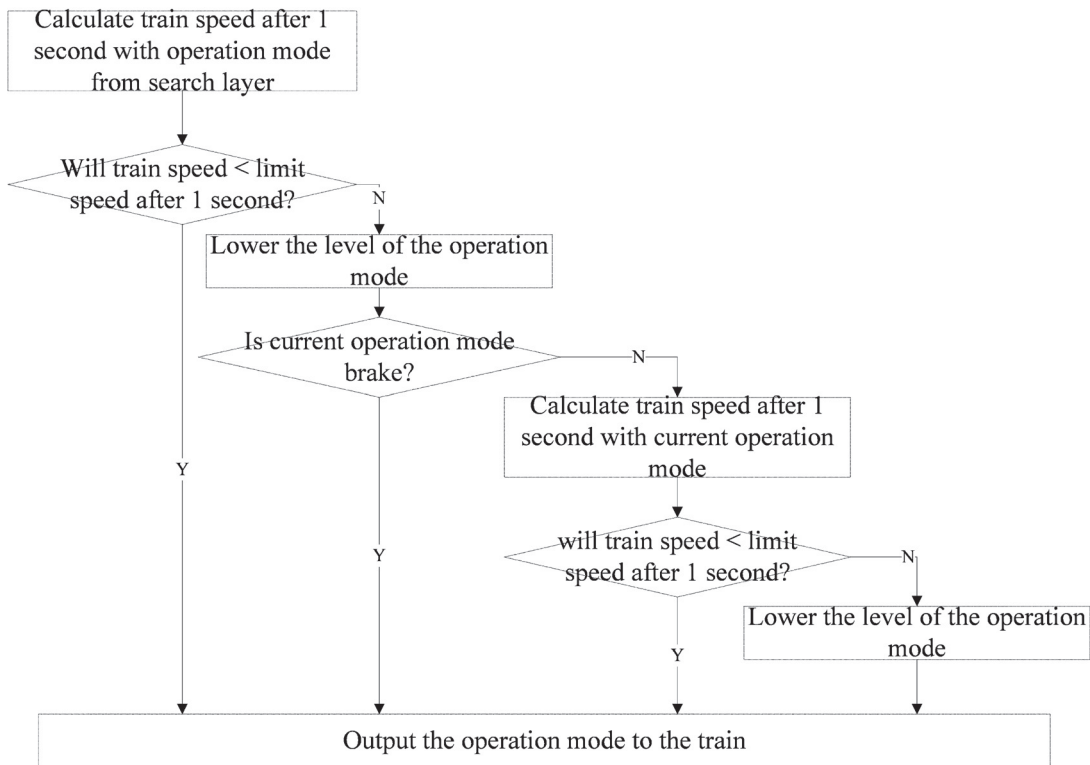


Figure 11 Work procedure of the protection layer.

Table 2 Parameters for multi-trains.

Parameter	Value
Train length	120 m
Safety margin	30 m
Length of the secure section	90 m
Headway	75 s

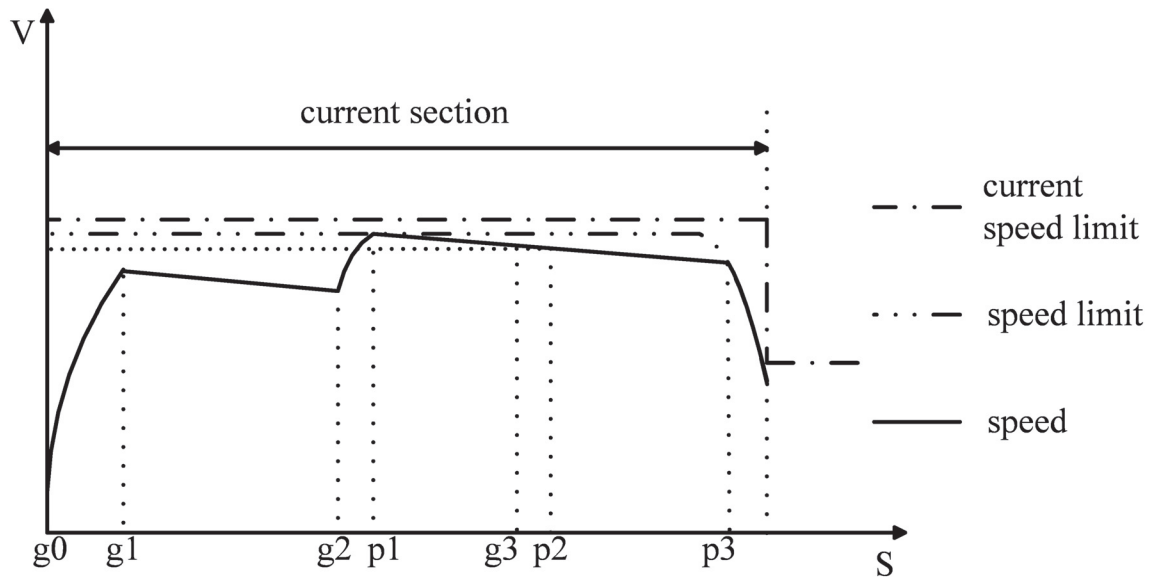


Figure 12 Control of the integrated ATO control algorithm.

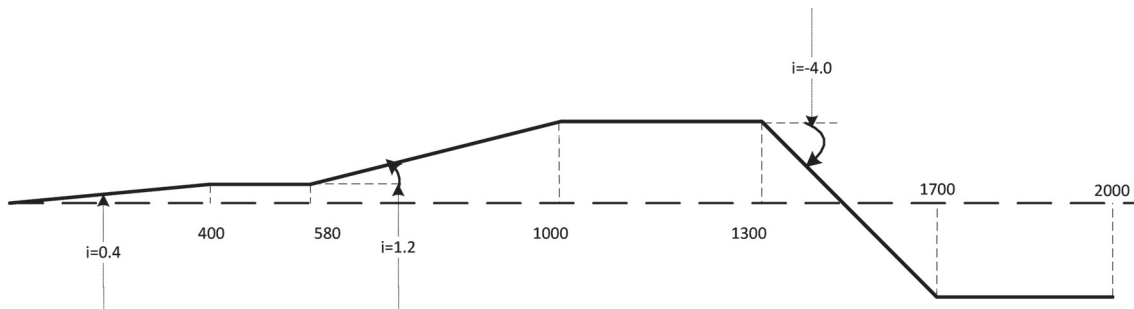


Figure 13 Gradient distribution.

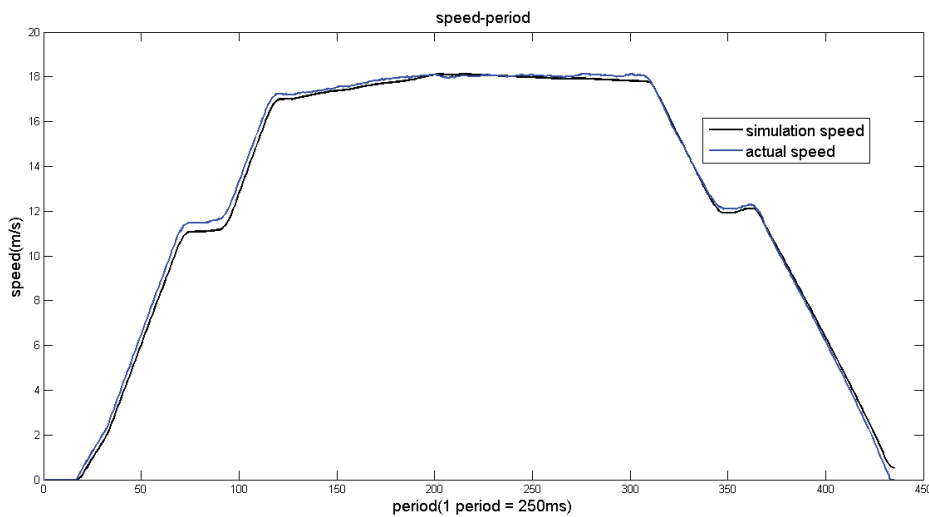


Figure 14 Simulation speed vs. actual speed.

We design a simulation line with a nonconstant gradient to create an actual simulation. The length of the simulation section is 2000 m, and the current speed limit is 22.2 m/s. The terminal point of the section is a temporary stop point whose speed limit is 0 m/s. The pure run time of the section is 116 s; thus, the schedule time is 133 s.

We study six types of operation strategies:

- Strategy 1, the flat-out operation strategy;
- Strategy 2, the control proportion is reduced;
- Strategy 3, both the traction proportion and the cruising speed are reduced;

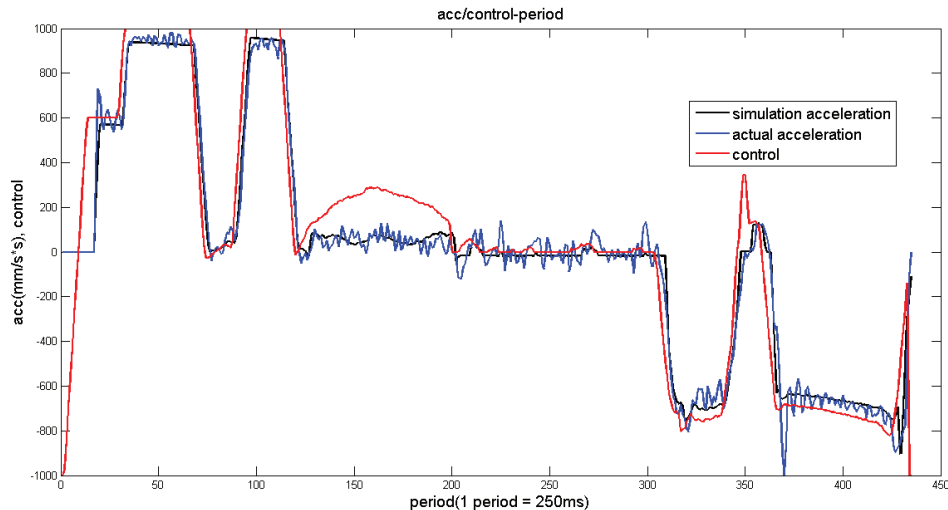


Figure 15 Simulation acc vs. actual acc vs. control.

- Strategy 4, only the cruising speed is reduced;
- Strategy 5, the proposed algorithm is applied.
- Strategy 6, the control proportion is reduced when the proposed algorithm is applied, which indicates that it reduces the control proportion in traction and braking control and applies a coasting and traction policy instead of a cruising policy.

With the exception of the flat-out operation strategy, other strategies guarantee the train to be punctual to the schedule. In the strategies that employ the cruising mode, the PID control is used to implement the cruise. In the simulation, the population of the GA is 40 and the maximum generation is 100. The speed-distance profiles of different strategies are shown in Figure 16. Figure 17–18 shows the speed-distance profile and information about the acceleration and operation mode for one train in a line and two trains in a line, respectively. Figure 19 shows the best fitness and average fitness of each generation. The optimal chromosome is [19 330, 99 397, 103 415], which indicates that the operation mode changes four times and coasting occurs at the point of 193.30 m, second traction occurs at 993.97 m and second coasting occurs at 1 034.15 m. The results of the six strategies are listed in Table 3.

The flat-out operation travels for 116 s and consumes 26.1583 kWh. Strategy 2 guarantees that the train will be punctual to the schedule by reducing the control proportion and consumes 25.8521 kWh, which is 98.8% of the flat-out operation. Strategy 2 performs poorly with regard to energy conservation because it needs equal energy to accelerate the train to the same cruising speed of Strategy 1. We discover that the full tractive power time of Strategy 1 accounts for 69% of Strategy 2, which corresponds to the value of the control proportion.

When we reduce the cruising speed in Strategy 3 and Strategy 4, the energy also decreases. The strategy with the lower cruising speed needs less full tractive power time and consumes less energy. Strategy 4 consumes the least amount of energy among the first four strategies using the maximum control proportion and the lowest cruising speed.

Strategy 6 performs well with regard to energy saving compared with strategy 2. Although it also reduces the control proportion by 30%, its full tractive power time decreases by 3.5 s and its energy consumption is only 18.8889 kWh. From this point, we can conclude that coasting and traction is superior to cruising with regard to energy saving.

Strategy 5, which employs the proposed algorithm, minimizes the energy consumption, although it uses 2.5 s longer of full tractive power time than Strategy 4, which suggests that the waste of energy during the cruising process is significant and can be eliminated using coasting mode. Considering that strategy 5 and strategy 6 are only different with regard to the control proportion, similar to strategy 1 and strategy 2, we discover that the full tractive power time of strategy 5 is 66% of strategy 6, which also approximately corresponds to the value of the control proportion. In addition, the comparison result indicate that the maximum control proportion consumes less energy.

With the maximum control proportion and optimum coast control, strategy 5 achieves the optimum energy-saving control.

## 5. CONCLUSIONS

This paper proposes an energy-saving ATO control algorithm that is based on a GA to solve the control problem of multi-train movements with incomplete information about speed limits. The algorithm is composed of two layers: the search layer, which employs a GA to search for the optimal control solution to determine the position where coasting should start or terminate; and the protection layer, which prevents the train from over-speed by degrading the operation mode when the train speed exceeds the speed limit. The chromosome of the GA has a variable length, which enables the algorithm to be more flexible in different situations of sections. The algorithm employs a novel fitness function to increase the survival rate of energy-efficient chromosomes. The simulation results indicate that the proposed algorithm can achieve the optimum energy-saving operation, which is also safe, punctual and comfortable. Future

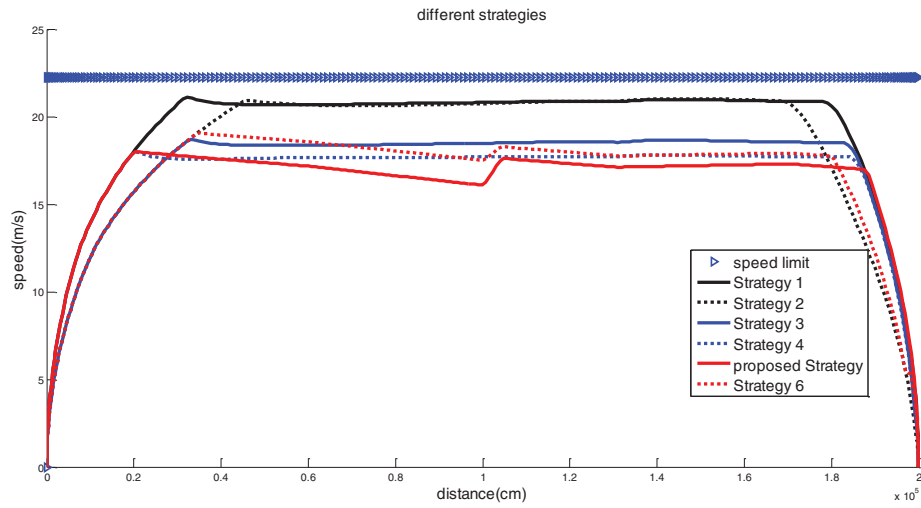


Figure 16 Speed-distance profiles of different strategies.

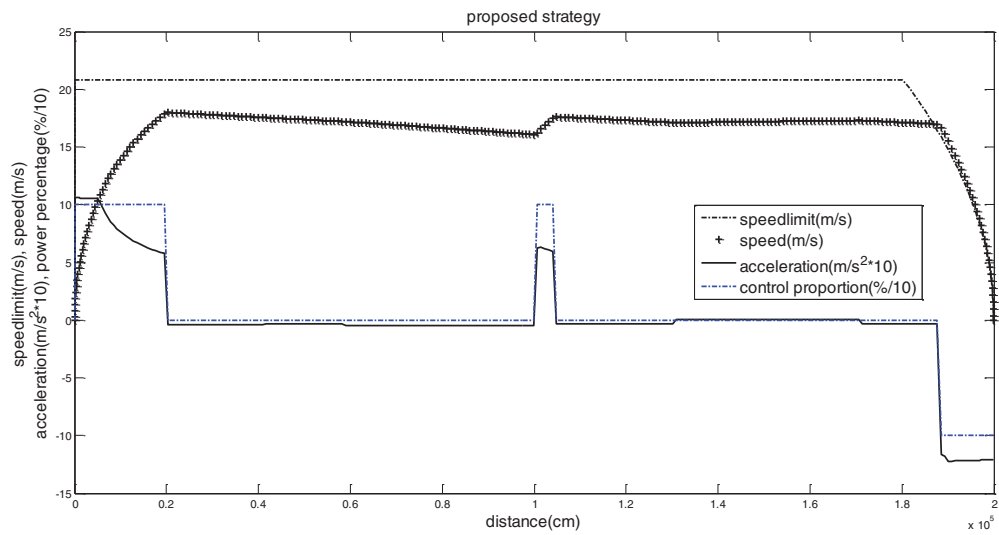


Figure 17 Simulation profiles of proposed strategy.

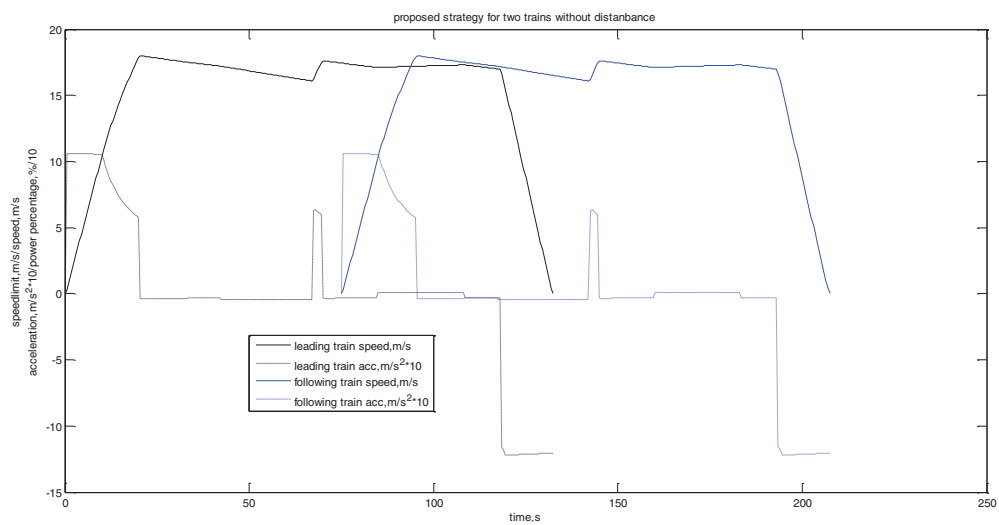


Figure 18 Simulation profiles of proposed strategy for two trains.

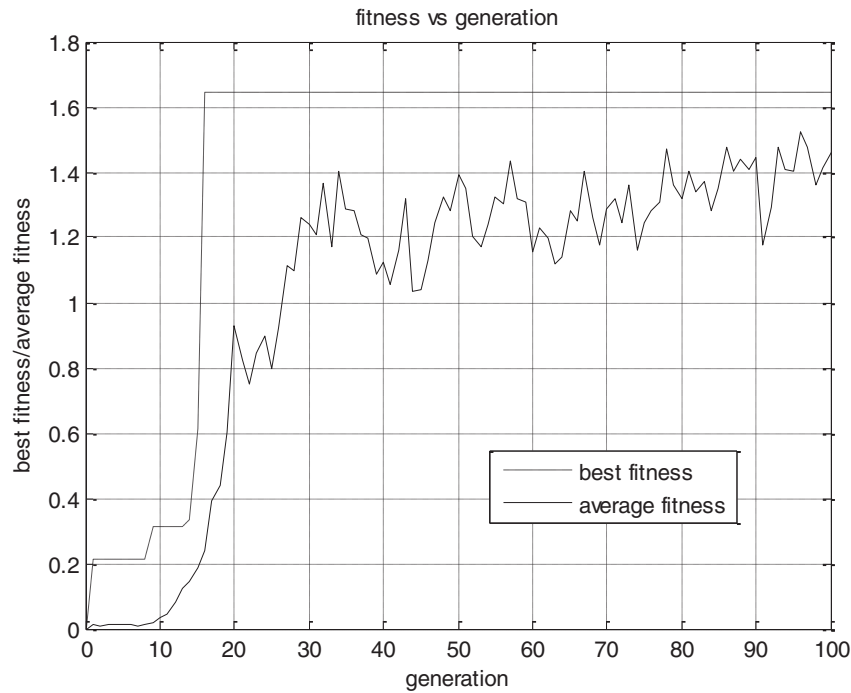


Figure 19 Fitness-generation profile.

Table 3 Results of the simulation.

	Strategy 1	Strategy 2	Strategy 3	Strategy 4	Proposed algorithm	Strategy 6
Travel dist (m)	1999.99	1999.89	1999.84	2000.01	1999.92	1999.76
Travel time (s)	116	132.5	133	133	132.5	133.5
Energy consumption (kWh)	26.1583	25.8521	21.2243	19.8840	17.4659	18.8889
Traction (%)	100	70	70	100	100	70
Brake (%)	100	70	100	100	100	70
Full tractive time (s)*	26	37.5	31	20	22.5	34
cruising speed (m/s)	20.8	20.8	18.5	17.7	/	/

\*full tractive time is the time when the permitted maximum tractive power is implemented.

research will focus on improving the efficiency of the algorithm and reducing energy consumption when trains are delayed.

### Acknowledgement

Comments and suggestions from the Editor and the referees are very much appreciated. This work is supported by the funding from the National Science and Technology Infrastructure Program of China under Grant 2011BAG01B03 and 2015BAG19B03.

### REFERENCES

1. Yi, W., Zhong, S. H., and Xing, Y. L. A novel automatic train operation algorithm based on iterative learning control theory. *Service Operations and Logistics, and Informatics*, **2008**. IEEE/SOLI 2008. IEEE International Conference, Beijing, China, Oct 2008, pp. 1766–1770.
2. Sekine, S., Imasaki, N., and Endo, T. Application of fuzzy neural network control to automatic train operation and tuning of its control rules'. *Fuzzy Systems*, **1995**. International Joint Conference

- of the Fourth IEEE International Conference on Fuzzy Systems and The Second International Fuzzy Engineering Symposium., Proceedings of **1995** IEEE International Conference, Yokohama, Japan, Mar 1995, pp. 1741–1746 vol. 4
3. Oshima, H., Yasunobu, S., and Sekino, S. Automatic train operation system based on predictive fuzzy control'. *Artificial Intelligence for Industrial Applications*, 1988. IEEE AI '88., Proceedings of the International Workshop, Hitachi City, Japan, May **1988**, pp. 486–486.
4. Bing, G., Hai, R. D., and Bin, N. Speed control algorithm for Automatic Train Operation Systems. *Computational Intelligence and Software Engineering*, 2009. CiSE 2009. International Conference, Wuhan, China, Dec **2009**, pp. 1–4.
5. Bing, G., Hai, R. D., and Yan, X. Z. Speed Adjustment Braking of Automatic Train Operation System based on Fuzzy-PID Switching Control. *Fuzzy Systems and Knowledge Discovery*, **2009**. FSKD '09. Sixth International Conference, Tianjin, China, Aug 2009, pp. 577–580
6. Chang, C. S., Xu, D. Y., and Quek, H. B. Pareto-optimal set based multi-objective tuning of fuzzy automatic train operation for mass transit system. *IEE Proceedings-Electric Power Applications*, **1999**, 146, (5), pp. 577–583

7. Chang, C. S., and Xu, D. Y. Differential evolution based tuning of fuzzy automatic train operation for mass rapid transit system. IEE Proceedings-Electric Power Applications, **2000**, 147, (3), pp. 206–212.
8. Seong, H. H., Yun, S. B., Jong, H. B., et al. An optimal automatic train operation (ATO) control using genetic algorithms (GA). TENCON 99. Proceedings of the IEEE Region 10 Conference, Cheju Island, South Korea, Sept **1999**, pp. 360–362 vol. 1
9. Chang, C.S., and Sim, S.S. Optimizing train movements through coast control using genetic algorithms. IEE Proceedings-Electric Power Applications, **1997**, 144, (1), pp. 65–73.
10. Bocharnikov, Y. V., Tobias, A. M., and Roberts, C. Optimal driving strategy for traction energy saving on DC suburban railways. IET-Electric Power Applications, **2007**, 1, (5), pp. 675–682.
11. Domínguez, M., Fernández, A., Cucala, A. P. and Lukaszewicz P. Optimal design of metro automatic train operation speed profiles for reducing energy consumption. Proc. IMechE, Part F: J. Rail and Rapid Transit **2011**, 225: 463–473.
12. Thomas Albrecht, Train Running Time Control Using Genetic Algorithms for The Minimization of Energy Costs in DC Rapid Transit Systems, Dresden University of Technology, Faculty of Traffic Sciences, **2004**.
13. Jörn, P. Railway operation and control (VTD Rail Publishing, 2009, 2nd edn.). Chapter 6.
14. Michalewicz, Z. Genetic Algorithms + Data Structures = Evolution Programs (Springer Publishing, **1996**, 3rd rev. and extended edn.).
15. Ming, H. T., Jian, Q. W., Guo, L. X. Composition of mass transit train and selection of traction motor. Electric Drive for Locomotives, **2005**, (5), pp. 50–53. [Chinese content, but English abstract].
16. Jin, J.F. Research of Train Traction Calculation System, Master Dissertation of Southwest Jiaotong University, chapter 3. [Chinese content, but English abstract].
17. Zhang, S, et al. Energy-efficient power allocation for MIMO two-way cognitive relay networks, Computer Systems Science and Engineering, **2015**, 30, 369–375.
18. Baek, J. The Study on train separation control and safety braking model technology using balise for conventional lines INTELEC 2009 - 31st International Telecommunications Energy Conference, **2009**, 1–4.
19. Baek, J., Lee, C. The Simulation of Train Separation Control Algorithm by Movement Authority Using Beacon, Fuzzy Systems and Knowledge Discovery, 2007. FSKD 2007. Fourth International Conference on, **2007**, 3, 717–720.
20. Gao, S.; Dong, H.; Ning, B.; Roberts, C. Neural adaptive coordination control of multiple trains under bidirectional communication topology, Neural Computing and Applications, **2015**, 1–11.
21. Takagi, R. Synchronization control of trains on the railway track controlled by the moving block signaling system. IET Electrical Systems in Transportation, **2012**, 2, 130–138.
22. Carvajal-Carreño W, et al. Fuzzy train tracking algorithm for the energy efficient operation of CBTC equipped metro lines. Engineering Applications of Artificial Intelligence, **2016**, 53, 19–31.
23. Ding, Y.; Bai, Y.; Liu, F. M. Simulation Algorithm for Energy-Efficient Train Control under Moving Block System. Computer Science and Information Engineering, 2009 WRI World Congress on, **2009**, 5, 498–502.
24. Gu, Q.; Lu, X. Y.; Tang, T. Energy saving for automatic train control in moving block signaling system. 2011 14th International IEEE Conference on Intelligent Transportation Systems (ITSC), **2011**, 1305–1310.
25. Wang, Y.; Schutter, B. D.; Ton, J.J. Optimal trajectory planning for trains under fixed and moving signaling systems using mixed integer linear programming. Control Engineering Practice, **2014**, 22, 44–56.
26. Carvajal-Carreño W, et al. A. Optimal design of energy-efficient ATO CBTC driving for metro lines based on NSGA-II with fuzzy parameters. Engineering Applications of Artificial Intelligence, **2014**, 36, 164–177.
27. Zeng, J.Q. The Research on Simulation System of EMU Traction Calculation, Master Dissertation of Beijing Jiaotong University, chapter 3. [Chinese content, but English abstract].
28. Wu, J. Energy efficient dual execution mode scheduling for real-time tasks with shared resources, Computer Systems Science and Engineering, **2016**, 31, 239–253.

## Appendix

### Notation

$\beta_{vt}$	Weight of $P_{vt}$
$\beta_s$	Weight of $P_s$
$\beta_t$	Weight of $P_t$
$\omega_1$	Weight of $E$
$\omega_2$	Weight of $VAR$
$E$	Energy consumption (kWh)
<i>fitness</i>	Fitness of a chromosome
$F_t$	Tractive force (kN)
$P_s$	Distance penalty
$P_t$	Punctuality penalty
$P_{vt}$	Speed penalty
$S$	Distance the train has travelled (cm)
$S_{\text{section}}$	Length of the section (cm)
$t$	Run-time of a train (s)
$t_{\text{section}}$	Schedule time of a section (s)
$V$	Train speed (m/s)
$V_{\text{ave}}$	Average speed (m/s)
$VAR$	variance index for the fitness function
$V_{\text{cruise}}$	Cruising speed of train to be punctual (m/s)
$V_{\text{CurrentLimit}}$	Current speed limit from the ATP system (m/s)
$V_{\text{margin}}$	Margin speed (m/s)
$V_t$	Train speed at the end of the section (m/s)
$V_{\text{TPLimit}}$	Speed limit of target point (m/s)

